Int J Adv Manuf Technol (2017) 93:2089–2096
DOI 10.1007/s00170-017-0665-7

ORIGINAL ARTICLE

Simulation analysis of ultrasonic detection for resistance spot welding based on COMSOL Multiphysics

Jing Liu[1] · **Guocheng Xu**[2] · **Lei Ren**[1,3] · **Zhihui Qian**[1] · **Luquan Ren**[1]

Received: 22 November 2016 / Accepted: 13 June 2017 / Published online: 26 June 2017

Abstract The simulated calculation is carried out on the ultrasonic detection process for stainless steel resistance spot welding by the finite element technology. It reveals the ultrasonic propagation characteristics and regularity in the inner of the spot welds, and provides a theoretical basis for selecting the Am as a characteristic parameter to represent the fusion state of the spot weld in the actual ultrasonic detection. Then the ultrasonic detection of spot welds with the presence of the porosity defect which easily appears is simulated, and the effect of the porosity on the ultrasonic propagation characteristics is studied. It is found that the ultrasonic reflection and transmission occur at the porosity defect, and finally the correctness and validity of the simulation and the model are verified by the experimental method.

Keywords Simulation analysis · Ultrasonic detection · Resistance spot welding · Porosity defect

✉ Lei Ren
jluliujing@126.com

✉ Zhihui Qian
zhqian@jlu.edu.cn

[1] Key Laboratory of Bionic Engineering, Ministry of Education, Jilin University, Changchun 130025, People's Republic of China

[2] Key Laboratory of Automobile Materials of Ministry of Education and Department of Materials Science & Engineering, Jilin University, Changchun 130025, People's Republic of China

[3] School of Mechanical, Aerospace and Civil Engineering, University of Manchester, M13 9PL, Manchester, UK

1 Introduction

Resistance spot welding is a welding method widely used in mechanical manufacturing of automobiles, etc. [1–3]. Since resistance spot welding joint is formed under closed condition, it becomes difficult to control and detect welding quality [4, 5]. Therefore, destructive testing method is adopted in the actual production to check the quality of spot welds of the test piece or the products being inspected. This method is not only inefficient but also wastes materials and energy. In recent years, with the continuous improvement of product quality requirements, nondestructive testing of spot welding quality has attracted more and more attention [6–8]. Spot welding ultrasonic nondestructive testing technology especially becomes a research hotspot at home and abroad with its advantages of convenience, reliability, and safety [9–11]. At present, the technology still has many urgent problems to be solved, such as the optimum detection parameters setting for different sample sizes and the qualitative and quantitative analysis of spot welding defects, which have greatly restricted its practical application.

Numerical simulation plays an important role in ultrasound spread studies as an effective analysis method [12–14]. Simulating ultrasonic testing process through finite element can not only deepen the understanding of the mechanism of ultrasonic echo but also design or optimize ultrasonic testing technology easily by changing the various detection parameters, which provide a theoretical basis for detection and reduce detection blindness [15, 16]. This article uses COMSOL Multiphysics simulation software to establish a simulation model of stainless steel resistance spot welding ultrasonic testing. The propagation characteristics of the sound field in different positions of the spot weld are simulated, and the methods of nugget edge recognition and quantitative calculation of nugget

diameter have been explored. At the same time, this article also simulates porosity defects which are liable to occur in welding nugget, and studies the influence of porosity defects on ultrasonic spread characteristics. It provides useful information for waveform analysis in the detection process, and has important theoretical and engineering significance in analyzing the relationship between the defect and the echo signal.

2 Basic theory of sound field simulation

Like ordinary sound waves, ultrasonic wave is the mechanical vibration in elastic medium in the form of fluctuation. Its spread process follows Newton's second law, the law of conservation of energy, and momentum conservation. Combining state equation of medium and small amplitude approximation, under the circumstance of ignoring physical power (external force acting on any unit volume of an object, such as its own gravity), the linear equation of the sound field in isotropic solid medium is expressed as

$$(\lambda + 2\mu)\nabla\nabla u - \mu\nabla \times \nabla \times u = \rho\frac{\partial^2 u}{\partial t^2} \quad (1)$$

where ρ is for medium density, u is for particle displacement, and λ and μ are for the lame constant.

The first step to simulate the ultrasonic detection process using the finite element method is the dispersion of the medium, that is, according to the requirements of the calculation precision and efficiency, the calculation area is divided into the mesh elements with a certain number and shape [17]. Then the displacement interpolation function is constructed, and the displacement of any node in the solution area is expressed by the node displacement and displacement interpolation function. Finally, the motion equation of the system is deduced from Eq. (1) by using the element analysis and Galerkin method combined with any characteristic of the node displacement variance [18]. If ignoring the influence of damping, the motion equation is simplified to

$$M\ddot{a}(t) + Ka(t) = Q(t) \quad (2)$$

where $\ddot{a}(t)$ and $a(t)$ are the systematic node acceleration vector and node velocity vector, respectively, and M, K, and Q(t) are, respectively, for the systematic mass matrix, stiffness matrix, and node load vector.

This paper uses stainless steel as the base material of the finite element model. The material parameters are as follows: Young's modulus $E = 210 \times 10^9$ Pa, Poisson's ratio $\sigma = 0.29$, density $\rho = 7930$ kg/m^3, and wavelength 0.42 mm. According to the material adopted in this paper, the measured sound velocity through a standard test block is $C_L = 5890.91$ m/s.

3 Establishment of simulation model

In this paper, COMSOL Multiphysics field coupling simulation software is used for the numerical simulation of stainless steel resistance spot welding ultrasonic testing. Since 3D model simulation calculation requires not only a higher computer hardware configuration but also a lot of computing time, a 2D model which limits appropriate boundary conditions is adopted in this paper to simulate 3D simulation calculation. At the same time, in order to further simplify the calculation, in the 2D simulation model, we set the spot weld to have the same material properties with the parent metal, only considering the effect of spot welding joint geometry characteristics on the sound field. According to the structural characteristics of stainless steel spot welding joint, the joint section model of the vertical detection plane is established in this paper, as shown in Fig. 1. In this model, the upper plate thickness is 1 mm and the lower plate thickness is 2 mm. The overall length is 10 mm. In the contact area of two layers of steel plate, a connecting area is set with a certain width as the size of the nugget diameter. The actual width of the joint section is far greater than 10 mm. So in the picture, the boundaries of 2, 5, 7, and 9 are artificial truncation boundaries, which are set as the damping boundary with certain absorption effect. The rest of 1, 3, 4, 6, 8, and 10 boundaries represent the actual outer surface of the steel plate. Considering the ultrasonic spread characteristics at the interface between steel and air, these boundaries are set as complete reflection boundaries.

3.1 Selection of drive signal

In this paper, transient drive pulse is used to simulate the ultrasonic wave, and the propagation characteristics of ultrasonic waves loaded vertically to the model surface are investigated. The drive signal is modulated through the corresponding Gaussian window function by adopting 2.5 cycle of the sine signal. The waveform is shown in Fig. 2. The signal center frequency is set to 15 MHz, and with reference to the actual probe diameter, the contact

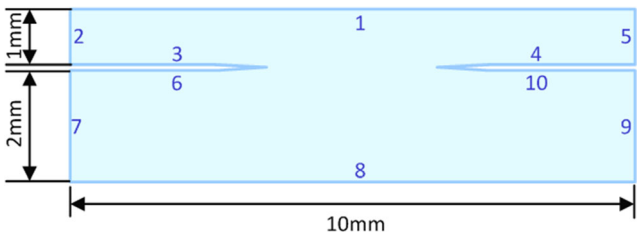

Fig. 1 Geometric model of the joint

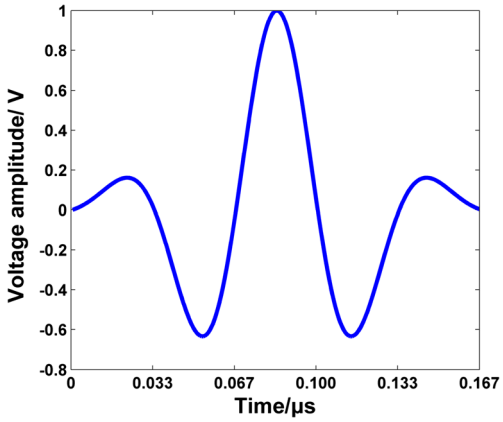

Fig. 2 Waveform graph of excitation signal

length of the drive signal which is loaded on model boundary 1 is set to 1 mm.

3.2 Mesh generations

Meshing is the vital step in the finite element numerical simulation, which directly affects the precision of numerical calculation. In dealing with the problem of acoustic wave, the principle of meshing is generally to control the largest cell size between 1/10 and 1/5 of the minimum wavelength. This principle can not only get enough high precision but also avoid the problems of slow solving speed caused by too-close meshing or the computer running out of memory. In this paper, free subdivision triangular mesh is adopted to divide the model. The largest cell size is 0.05 mm. After construction, the total cell of the model is 31,178. The number of degree of freedom is 63,157.

4 Simulation calculation result and analysis

4.1 Simulation analysis of ultrasonic detection echo signal of spot welding joint

When the ultrasonic probe is located in the parent metal area of the spot welding joint, the interior sound field transient distribution simulation results are as shown in Fig. 3. From the diagram, it can be seen that the ultrasonic wave incidents to the underside of the upper plate indeed all reflect. And the ultrasonic echo is not affected by the nugget area. Specular reflection just happens on the surface of the upper plate. Figure 4 is the corresponding A-echo signal simulation waveform figure. It can be seen from the table that the once-echo amplitude Am of the bottom of the upper plate is bigger. The distance between wave crests is the sound path of the upper plate thickness, and the sound wave shape and the beam direction has not been changed.

When the ultrasonic probe is located in the welding joint bonding line area, the interior sound field transient distribution simulation results are as shown in Fig. 5. When the incident sound wave reaches the lower surface of the upper steel plate, the sound wave diffraction happens in the cutting edge of the bonding line, and spread all around, centered on the cutting edge. Only part of the sound waves are received by the probe, causing the once-echo amplitude Am of the bottom of the upper plate to be reduced, as shown in Fig. 6. In the later spread process, diffraction happens when ultrasound passes the cutting edge of the bonding line every time, causing the A-echo signal to attenuate rapidly.

When ultrasonic probe is located in the spot welding nugget area, the simulation result of internal sound field transient distribution is as shown in Fig. 7. Almost all ultrasonic waves penetrate through the nugget, and reflect at the bottom of the

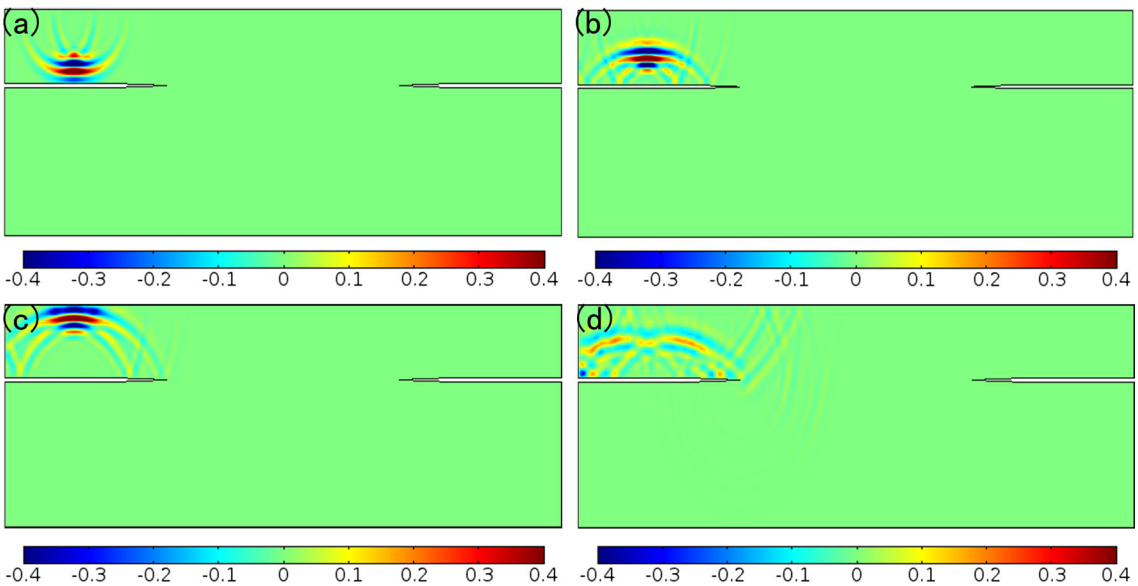

Fig. 3 Transient internal acoustic field distribution diagram of base metal. **a** 0.2 μs. **b** 0.31 μs. **c** 0.39 μs. **d** 0.69 μs

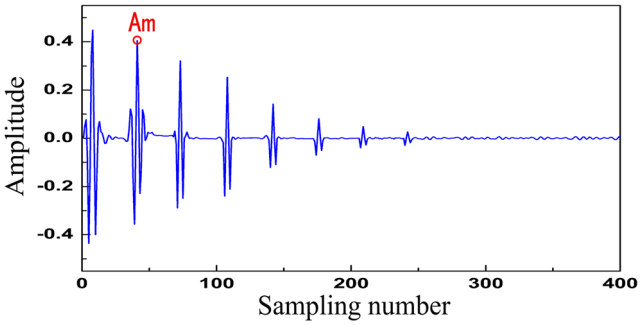

Fig. 4 A-echo signal simulation waveform

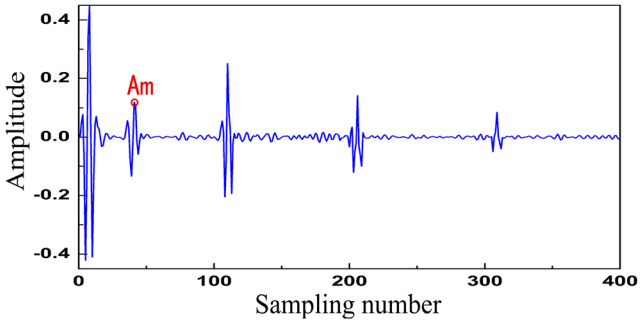

Fig. 6 A-echo signal simulation waveform

lower plate. The sound path is three times the echo at the bottom of the upper plate. And the Am is close to the lowest at this time, as shown in Fig. 8. When the reflected wave at the bottom of the lower plate passes through the fusion area, a small amount of sound wave diffracts at the edge of the bonding line. And in the process of later spread, the signal of the diffracted wave and reflected wave or transmitted wave overlaps partly, and interferes with the ultrasonic echo, resulting in glasslike noise, which can be reflected in the A-echo signal waveform graph (Fig. 8).

The simulation results show that A-echo at different locations of the welding joint has respective characteristics. The once-echo amplitude Am at the bottom of the upper plate changes obviously. It provides a theoretical basis for the selection of Am as the characteristic parameter of the internal fusion state of the joint in practical welding ultrasonic detection [19–21].

4.2 Simulation results of porosity defect

Ultrasonic detection simulation has been carried out on porosity defect which frequently appears in stainless steel welding nugget to study porosity's influence on ultrasonic spread characteristics. When the porosity defect is 2 mm away from the lower surface and its diameter is 0.06 mm within the spot welding joint, the transient distribution of the sound field inside the joint is as shown in Fig. 9. In the picture, it can be seen that in the process of propagation in the stainless steel medium, ultrasound reflection and transmission occur at the porosity. When the time is 0.33 μs, the reflection echo of the defect arrives at the coupling place between the probe and the workpiece. The transmitted wave continues to spread to the lower plate, and reflection occurs at the bottom of the lower plate. The once-echo at the bottom of the lower plate returns along the original path and it arrives at the probe at 1.03 μs. The ultrasonic A-scan waveform diagram is obtained by means of echo signal superposition at each point on the surface of the sound source characterizing received signal, as shown in Fig. 10. It can be seen from the diagram, at one third position between the surface wave and the lower steel plate bottom echo, that the reflection echo of the porosity defect appears, which is in good agreement with the position of porosity defect in the simulation model. And the influence of porosity defect on ultrasonic reflection and scattering causes the

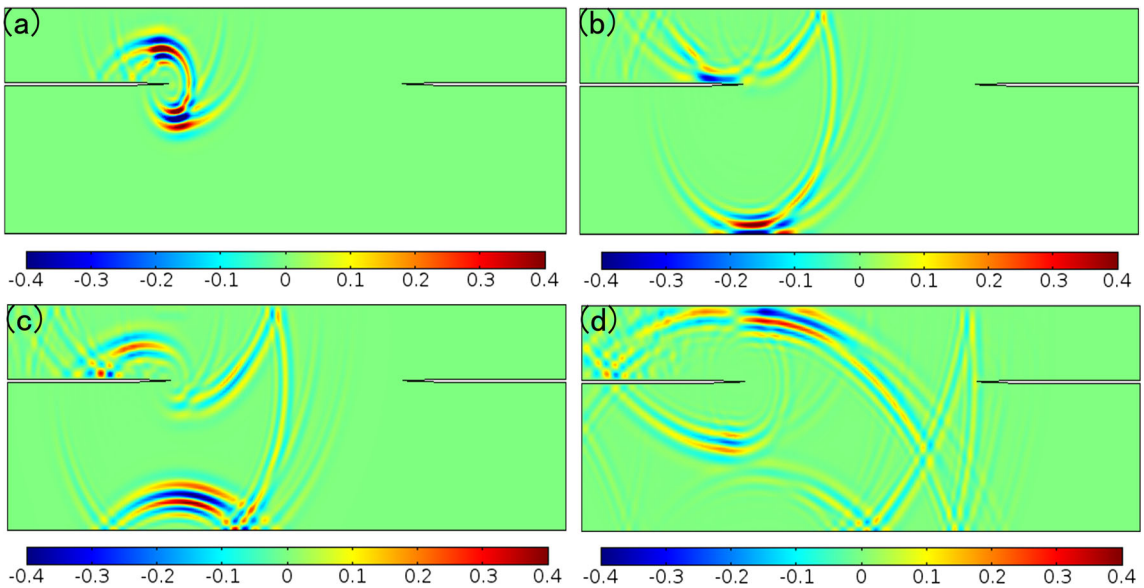

Fig. 5 Transient internal acoustic field distribution diagram of combination line. **a** 0.33 μs. **b** 0.6 μs. **c** 0.69 μs. **d** 1.33 μs

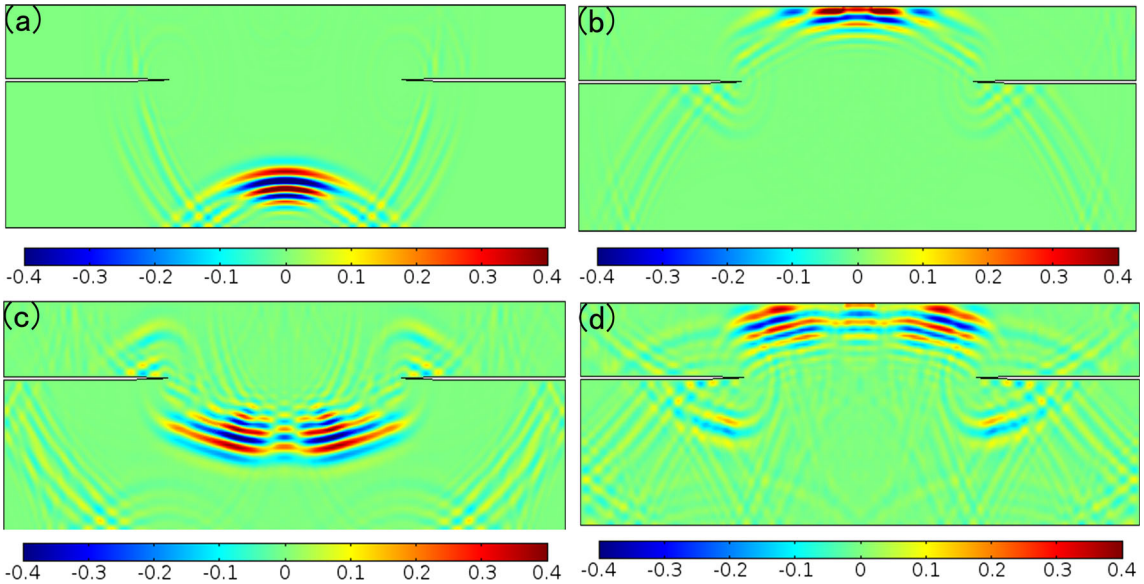

Fig. 7 Transient internal acoustic field distribution diagram of the nugget. **a** 0.72 μs. **b** 1.16 μs. **c** 1.5 μs. **d** 2.23 μs

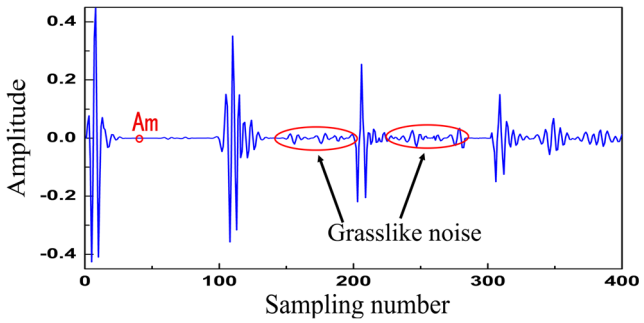

Fig. 8 A-echo signal simulation waveform

reflection echo to have obvious attenuation on the surface of the steel plate.

For further study on the influence rule of porosity defect on ultrasonic spread characteristics, this paper sets up porosity defects with different depths to observe the effect on ultrasonic detection and obtain the corresponding ultrasonic detection A-scan waveform, as shown in Figs. 11 and 12. It can be seen from the diagram, similar to the porosity depth of 2 mm, that ultrasonic wave reflection and transmission occur at the porosity. With the change of the porosity location, defect

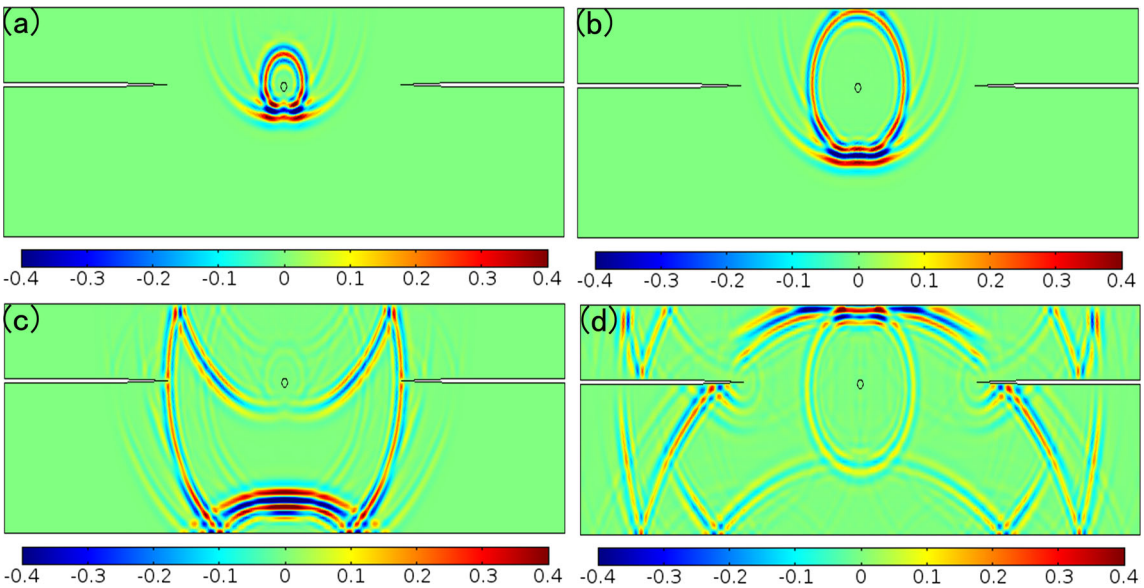

Fig. 9 Transient internal acoustic field distribution diagram of the joint with porosity depth of 2 mm at different times. **a** 0.22 μs. **b** 0.33 μs. **c** 0.57 μs. **d** 1.03 μs

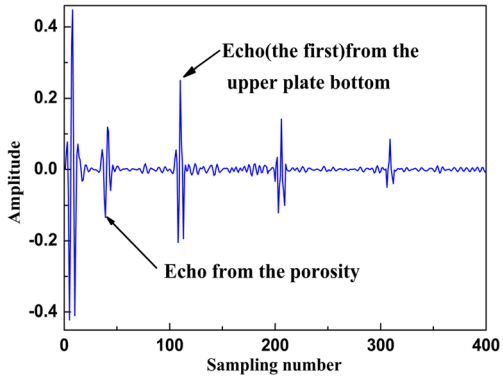

Fig. 10 A-scan waveform of ultrasonic detection

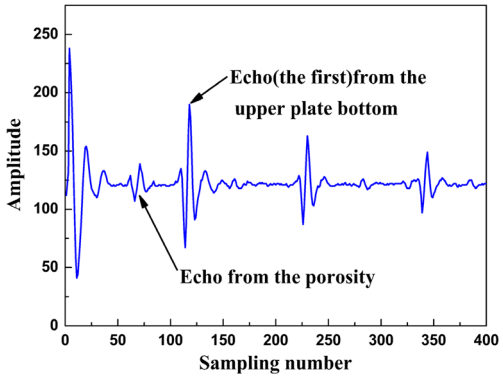

Fig. 13 Typical A-scanning waveform of defects

reflection echo moves therewith, and it is in good agreement with the position of the porosity defect in the simulation model.

5 Experimental verification

By adjusting the welding parameters and welding conditions, a large number of spot welded specimens with porosity defects were prepared. A 15 MHz high-frequency focusing probe is adopted to scan and detect. The typical A-scan waveform at the defection place is shown in Fig. 13. Compared with the simulation results in Fig. 10, the defect echo amplitude is small. This is because the ultrasonic absorption and scattering of bulky organization within the actual spot welding nugget is large. However, the simulation model uses the simplified form, ignoring the attenuation caused by multiple scattering of actual material internal organization and grain boundary. At the same time, the noise of test and limited width of the sample are also the reasons causing the difference between the actual testing results and the simulation results. But for the signal main part, that is, the ultrasonic echo amplitude and phase, the actual detection keeps good consistency with the simulation results. The once-echo amplitude Am at the bottom of the upper plate is used as a characteristic parameter representing a joint internal fusion state, and the C-scan

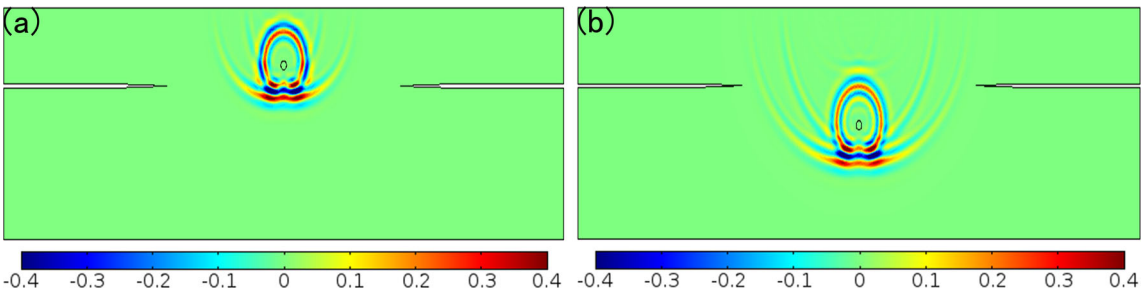

Fig. 11 Transient internal acoustic field distribution diagram of the joint with different porosity depth. **a** Porosity depth is 2.3 mm. **b** Porosity depth is 1.5 mm

Fig. 12 A-scan waveform of ultrasonic detection. **a** Porosity depth is 2.3 mm. **b** Porosity depth is 1.5 mm

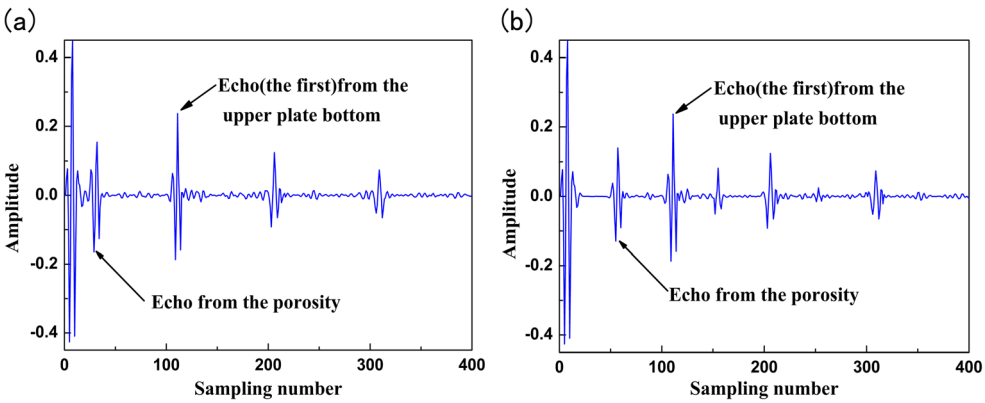

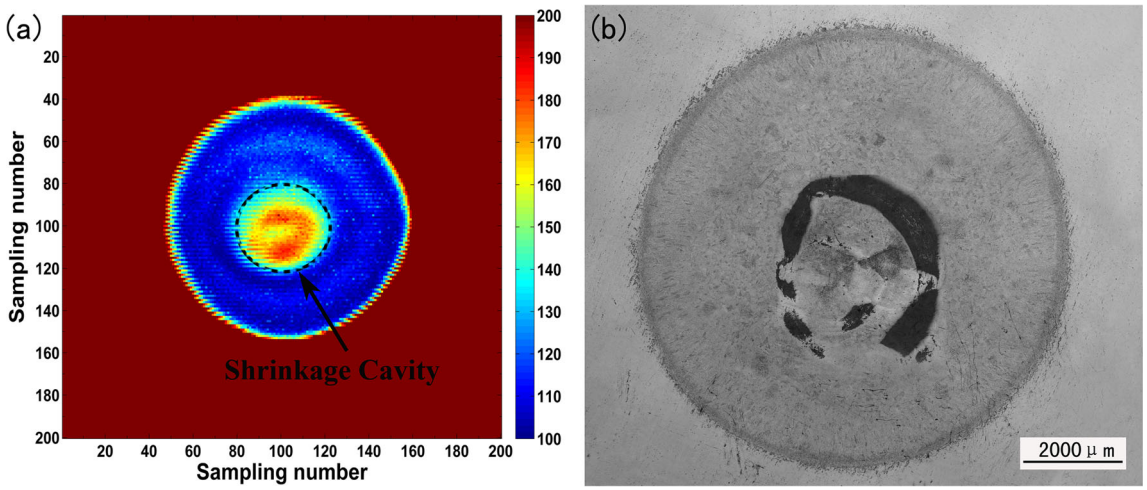

Fig. 14 Diagrams of spot welded specimen. **a** C-scan diagram. **b** The joint cross-section metallograph

image of the whole scanning area is obtained. One of the C-scan images of spot welded specimens is shown in Fig. 14a, and the corresponding cross-section metallograph is shown in Fig. 14b. It can be seen from the figure that the shape of the nugget and porosity are very close in the detecting image and real metallograph.

The accuracy of ultrasonic test of the nugget diameter and porosity defects is also further studied in this article. A comparison diagram of ultrasonic testing values and metallographic test values of 12 spot welding specimens is shown in Fig. 15, where De refers to the ultrasonic testing value of the nugget diameter, Dm refers to the metallographic measured value of the nugget diameter, Se refers to the ultrasonic testing value of porosity, and Sm refers to the metallographic measured value of porosity. The ultrasonic testing values of the nugget diameter and porosity are in good agreement with the measured values, and the average relative error is 1.069 and 4.827%, respectively, which can meet the requirement of industrial detection accuracy. Therefore, the method of simulation analysis of ultrasonic detection for resistance spot welding based on COMSOL Multiphysics has a high accuracy.

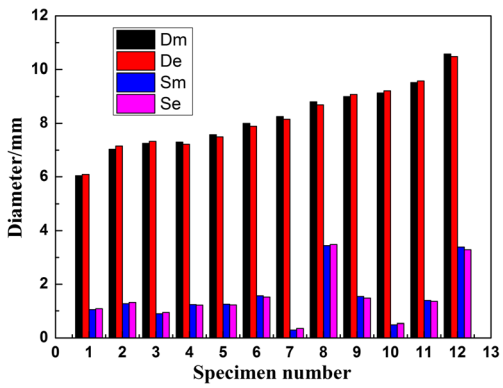

Fig. 15 Comparison diagram of ultrasonic testing values and metallographic test values

6 Conclusions

In this paper, COMSOL Multiphysics software is used to simulate the process of the ultrasonic detection of spot welds. The results show that the A-scan waveform at different locations of the spot weld has respective characteristics. The amplitude value Am of the once-echo from the upper plate bottom changes obviously in particular, which provides a theoretical basis for selecting the Am as a characteristic parameter to represent the fusion state of the spot weld in the actual ultrasonic detection.

The ultrasonic detection of spot welds with the presence of the porosity defect is simulated, and the effect of different depths of the porosity on the ultrasonic propagation characteristics is studied. It is shown that the ultrasonic wave is reflected and transmitted at the porosity, and with the change of the porosity location, the defect echo also moves.

Through the verification test, it is found that the amplitude value and phase of the actual ultrasonic echo are consistent with the simulation results. The ultrasonic testing values of the nugget diameter and porosity are in good agreement with the measured values, and the average relative error is 1.069 and 4.827%, respectively, which can meet the requirement of industrial detection accuracy, and then prove the correctness and validity of the simulation model and the method used in this paper.

Acknowledgements This research was supported by the project of the National Natural Science Foundation of China (No. 51475202 and No. 51675222), the project of Postdoctoral Science Foundation of China (No. 2016M601381), and the project of the scientific and technological cooperation between China and Italy (No. 2016YFE0103700).

References

1. Min J (2003) Real time monitoring weld quality of resistance spot welding for the fabrication of sheet metal assemblies. J Mater Process Technol 132(1–3):102–113. doi:10.1016/S0924-0136(02)00409-0
2. Bina MH, Jamali M, Shamanian M, Sabet H (2014) Investigation on the resistance spot-welded austenitic/ferritic stainless steel. Int J Adv Manuf Technol 75(9):1371–1379. doi:10.1007/s00170-014-6220-x
3. Podržaj P, Simončič S (2011) Resistance spot welding control based on fuzzy logic. Int J Adv Manuf Technol 52(9):959–967. doi:10.1007/s00170-010-2794-0
4. Luo Y, Liu JH, Xu HB, Xiong CZ, Liu L (2009) Regression modeling and process analysis of resistance spot welding on galvanized steel sheet. Mater Des 30(7):2547–2555. doi:10.1016/j.matdes.2008.09.031
5. Wan XD, Wang YX, Zhao DW (2016) Quality monitoring based on dynamic resistance and principal component analysis in small scale resistance spot welding process. Int J Adv Manuf Technol 86(9):3443–3451. doi:10.1007/s00170-016-8374-1
6. Zhang HJ, Hou YY, Zhang JY, Qi XY, Wang FJ (2015) A new method for nondestructive quality evaluation of the resistance spot welding based on the radar chart method and the decision tree classifier. Int J Adv Manuf Technol 75(5):841–851. doi:10.1007/s00170-014-6654-1
7. Ruisz J, Biber J, Loipetsberger M (2007) Quality evaluation in resistance spot welding by analysing the weld fingerprint on metal bands by computer vision. Int J Adv Manuf Technol 33(9):952–960. doi:10.1007/s00170-006-0522-6
8. Chertov AM, Maev RG, Severin FM (2007) Acoustic microscopy of internal structure of resistance spot welds. IEEE T Ultrason Ferr 54(8):1521–1529. doi:10.1109/TUFFC.2007.422
9. Moghanizadeh A (2016) Evaluation of the physical properties of spot welding using ultrasonic testing[J]. Int J Adv Manuf Technol 85(1):535–545
10. El-Banna M, Filev D, Chinnam RB (2008) Online qualitative nugget classification by using a linear vector quantization neural network for resistance spot welding. Int J Adv Manuf Technol 36(3):237–248. doi:10.1007/s00170-006-0835-5
11. Liu J, Xu GC, Ren L, Qian ZH, Ren LQ (2016) Defect intelligent identification in resistance spot welding ultrasonic detection based on wavelet packet and neural network. Int J Adv Manuf Technol 90(9):2581–2588. doi:10.1007/s00170-016-9588-y
12. Declercq NF, Degrieck J, Leroy O (2006) Ultrasonic polar scans: numerical simulation on generally anisotropic media. Ultrasonics 45:32–39. doi:10.1016/j.ultras.2006.05.219
13. Javadi Y, Akhlaghi M, Najafabadi MA (2013) Using finite element and ultrasonic method to evaluate welding longitudinal residual stress through the thickness in austenitic stainless steel plates. Mater Des 45:628–642. doi:10.1016/j.matdes.2012.09.038
14. Ben BS, Yang SH, Ratnam C, Ben A (2013) Ultrasonic based structural damage detection using combined finite element and model Lamb wave propagation parameters in composite materials. Int J Adv Manuf Technol 67(5):1847–1856. doi:10.1007/s00170-012-4613-2
15. Ke W, Castaings M, Bacon C (2009) 3D finite element simulations of an air-coupled ultrasonic NDT system. NDT & Int 42(6):524–533. doi:10.1016/j.ndteint.2009.03.002
16. Song YK, Hua L, Wang XK, Wang B, Liu YL (2016) Reasearch on the detection model and method for evaluating spot welding quality based on ultrasonic A-scan analysis. J Nondestruct Eval 35(1):1–12. doi:10.1007/s10921-015-0319-3
17. Baskaran G, Rao CL, Balasubramaniam K (2007) Simulation of the TOFD technique using the finite element method. Insight 49(11):641–646. doi:10.1784/insi.2007.49.11.641
18. Belytschko T, Lu YY, Gu L (1994) Element-free Galerkin methods. Int J Numer Meth Eng 37:229–256. doi:10.1002/nme.1620370205
19. Liu J, Xu GC, Gu XP, Zhou GH, Hao YK (2014) Ultrasonic C-scan detection for stainless steel spot welds based on signal analysis in frequency domain. ISIJ Int 54(8):1876–1882. doi:10.2355/isijinternational.54.1876
20. Fujita MM, Ueno MM, Iwamoto C, Satonaka S (2013) Ultrasonic evaluation of spot welding nugget diameter with a line-focused probe. Weld World 53(11):281–289. doi:10.1007/BF03263471
21. Thornton M, Han L, Shergold M (2012) Progress in NDT of resistance spot welding of aluminium using ultrasonic C-scan. NDT & Int 48(2):30–38. doi:10.1016/j.ndteint.2012.02.005